TIME-RESOLVED PHOTOLUMINESCENCE STUDIES ON HIGH ALUMINIUM COMPOSITION AlGaN EPILAYER

W. LI[1], W. Y. WANG[2], D. F. MAO[2], P. JIN[2]

AlGaN epitaxial layer has been studied by means of temperature dependent time-integrated photoluminescence (PL) and time-resolved photoluminescence (TRPL). A relatively slow rising stage in the rising stage of fluorescent decay curves was observed at 70K. Radiative recombination lifetime increases linearly with temperature during the low temperature range. Also, an anti-S-shaped temperature dependence of radiative recombination lifetime of carriers was observed. We demonstrate that these behaviors are caused by a change in the carrier dynamics with increasing temperature due to the competition of carriers' localization and delocalization in the AlGaN alloy.

Keywords: AlGaN, time-resolved photoluminescence, carrier dynamics

1. Introduction

Due to the band gap varying from 3.4 to 6.2 eV, AlGaN ternary compound has attracted much interest and is widely used in light emitting devices [1,2], high power and high temperature electronic devices [3,4]. Meanwhile, high Al composition $Al_xGa_{1-x}N$ ($x>0.4$) material is an ideal compound alloy for realizing the luminescence and detection at the solar blind region [5,6]. However, due to the lattice mismatch and thermal mismatch, high Al composition $Al_xGa_{1-x}N$ suffers from high density of threading dislocations, which act as nonradiative recombination centers. In the previous reports about the AlGaN localized states, several groups [7-13] have studied the AlGaN localized states by means of time-integrated photoluminescence (PL) or time-resolved photoluminescence (TRPL) and they all hold the point that the "S" shaped PL peak energy was caused by band tail state due to the alloy fluctuation in AlGaN alloy. Some authors [7, 8] pointed out that carrier's localization was favorable for efficient light emission due to preventing the nonequilibrium carriers from reaching the nonradiative recombination centers. Although many researchers have reported carriers localization induced by potential fluctuations in AlGaN epilayers, the variation of carriers transferring with increasing temperature is not fully understood. For the optoelectronic devices, it is the dynamic processes of the optical transitions that

[1] Science and Technology on Metrology and Calibration Laboratory, Changcheng Institute of Metrology & Measurement, Aviation Industry Corporation of China, Beijing, China, e-mail: livy09@163.com

[2] Key Laboratory of Semiconductor Materials Science, Institute of Semiconductors, College of Materials Science and Opto-Electronic Technology, University of Chinese Academy of Sciences, Chinese Academy of Sciences, Beijing, China, e-mail: weiying@163.com

predominantly determine their performance. A further exploring and understanding of the carrier's dynamics of the AlGaN alloys are useful for improving sample quality as well as immense value in designing and optimizing optoelectronic devices.

In this work, we report temperature-dependent PL studies of high Al composition $Al_{0.6}Ga_{0.4}N$ by means of time-integrated PL and TRPL. We show the variation of temperature dependent PL peak energy and exhibit temporal responses of the PL emission at various temperatures. Also, we demonstrate the effect of carriers transferring on the rising stage of fluorescent decay curve and analyze the variation of radiative recombination lifetime as well as nonradiative recombination lifetime as temperature increased. By combining the steady-optical measurements results with temporal response results, excitons recombination dynamics are analyzed.

2. Experimental part

AlGaN epilayer with a thickness of 2 μm was grown on c-plane sapphire films by metalorganic chemical vapor deposition (MOCVD). Trimethygallium (TMG), trimethylaluminium (TMAl), and ammonia were used as precursors in the AlGaN growth. H_2 was used as a carrier gas. Prior to the AlGaN growth, a 50-nm low-temperature AlN nucleation layer and a 1.0 μm AlN template were grown. The composition of the AlGaN epitaxial layer was determined by X-ray diffraction (XRD) measurements, the Al content was calculated from the c lattice parameter assuming the Vegard's law and was estimated to be 60%. PL measurement was performed by a home-made vacuum spectroscope, Fig. 1 shows the schematic description of the vacuum spectroscope.

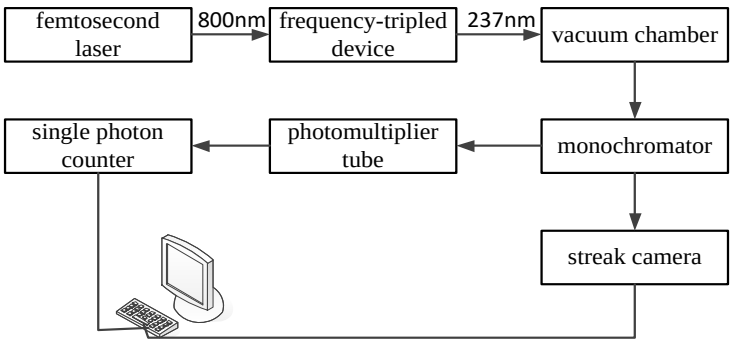

Fig. 1. Schematic description of the vacuum spectroscope

The excitation source was frequency-tripled mode-locked Ti: sapphire femtosecond laser, with an excitation wavelength of 237 nm. The sample was mounted on a copper panel with a cold finger in a closed-cycle helium refrigerator. The temperature range of our measurements was from 10 K to 300 K.

For the continuous wave PL measurements, the PL was dispersed with a monochromator and detected by the photomultiplier tube together with a single photon counting detection system. For the TRPL measurements, the PL was dispersed with a monochromator and detected by a stand streak camera acquisition system, and the overall time resolution of the laser spectroscopic system is less than 16 ps.

3. Results and Discussion

Fig. 2 shows the low temperature PL spectra of $Al_{0.6}Ga_{0.4}N$ epilayer at 10 K. A main PL emission denoted as E_{P1} at 4.995 eV was observed. E_{P1} shows an "s" shaped PL peak energy as temperature increases. At the low energy side of E_{P1}, there are two weak peaks at about 4.850 and 4.746 eV, respectively. These two peaks are denoted as $E_{P2,}$ and E_{P3}, respectively. We note that the energy separation between the successive three peaks is about 105 meV, Since the longitudinal optical (LO) phonon replicas in GaN and AlN are 92 and 110 meV, [14, 15] respectively, we believe the transition peak of E_{P1} is due to the recombination of localized excitons, and the transition peaks of E_{P2} and E_{P3} are assigned to the n = 1 and n = 2 LO phonon replicas of the localized excitons.

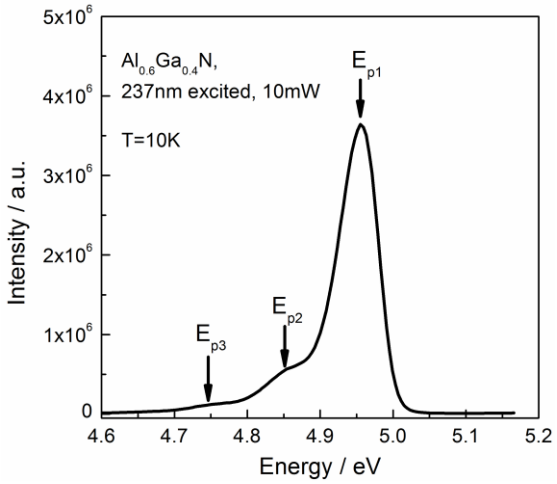

Fig. 2. PL spectra of $Al_{0.6}Ga_{0.4}N$ epilayer measured at 10 K

The S-shaped temperature dependent variation of E_{P1} is showed in Fig. 3, the peak of localized excitons decreases in the temperature range of 10-30 K, increases for 30-70 K, and decreases again for 70-240 K. The S-shaped dependence of PL peak energy on temperature is commonly observed and is a well-known manifestation of nonthermalized to thermalized distribution of localized excitons. [8-10] the initial redshift is caused by redistribution of excitons to lower localized states, and the blueshift is attributed to excitons beginning to occupy different higher energy states due to increasing thermal energy, while the

subsequent redshift is due to the typical band gap shrinkage with temperature.

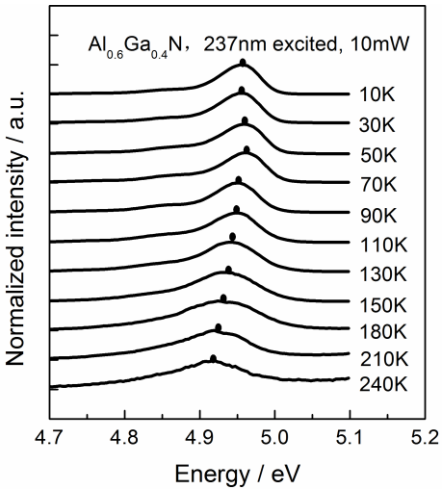

Fig. 3 Temperature dependence of PL spectra of $Al_{0.6}Ga_{0.4}N$ epilayer from 10 to 240 K. All spectra are normalized and shifted in the vertical direction for clarity.

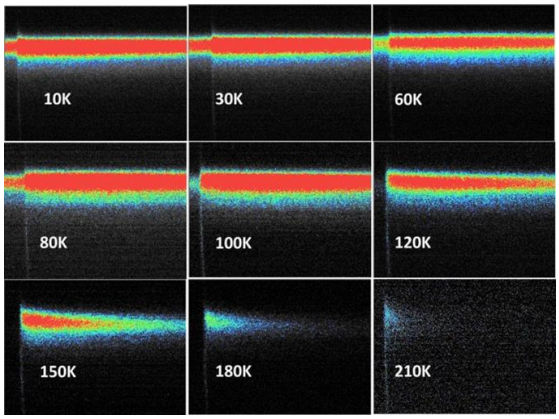

Fig. 4 Images captured by streak camera at different temperature

Fig. 4 demonstrates the images captured by the streak camera at various temperatures, all of the images are taken in the same conditions. For the images taken by the streak camera, the horizontal axis denotes time and the unit is picosecond, the vertical axis is corresponding with wavelength and the unit is nanometer. The brightness of the images signifies the fluorescence intensity, and the fluorescence intensity is a function of time and wavelength. Intuitively, the fluorescence intensity is strong and lasts long at low temperature, the intensity and lasting time all decrease as temperature increases. We scratched the data at the center wavelength which was corresponding to the peak energy along the horizontal axis, and then we obtained the decay curves at different temperature. Fig. 5 shows the decay spectra of E_{P1} at some representative temperature. All decay curves can be divided into two parts, the fluorescent rising stage and the

fluorescent declining stage. For the fluorescent rising stage, we note that the rising stage is relatively sharp at 10 K, and a relatively slow rising stage at 70 K, then the slow rising stage is weak at 110 K, and the rising stage return to relatively sharp at 150 K. This phenomenon can be understood in this way, the rising stage of fluorescent decay curve denotes the process of carriers relaxation, for T = 10 K, the relatively sharp rising stage indicates that the carriers relaxation process is very fast, carriers transferring between different localized states is weak due to the low temperature. For T=70 K, the thermal energy of carriers increased with enhancing temperature, carriers begin to occupy different higher energy states, and we can see the blueshift in the time-integrated PL. At the same time, the time of carrier's relaxation process is extended due to carriers transferring, so there is an obviously slow rising stage at 70 K. For T=110 K, part of carriers is still in the localized and there is carriers transferring in the localized states, part of carriers escape from localized states quickly due to the enhanced thermal energy, so compared with 70 K, the slow rising stage was weaker at 110 K. For T=150 K, most carriers escape from localized states quickly due to the higher thermal energy, so the rising stage return to relatively sharp at 150 K. The declining stage of fluorescent decay curve denotes the process of carrier's recombination. We can get the information of carriers recombination dynamics through the analysis of the declining stage of fluorescent decay, all the fluorescent declining stage can be well fitted with monoexponential curve:

$$I(t) = A\exp(-t/\tau_{\text{eff}}), \tag{1}$$

where *I(t)* is the PL intensity at time *t*, *A* is a proportional coefficient, τ_{eff} represents the effective recombination lifetime which can be obtained by fitting the decay curves using the monoexponential curve.

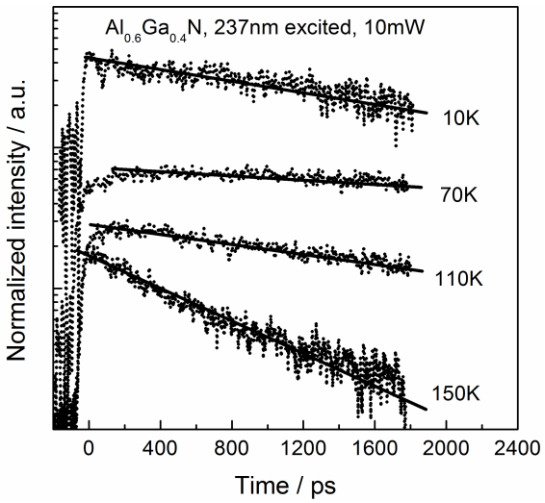

Fig. 5. Temperature dependent TRPL transients of E_{P1} measured at the corresponding peak energy for the $Al_{0.6}Ga_{0.4}N$ epilayer

The dotted line is the experiment data while the solid line is the fitting curve according to Eq. (1). To explore the dynamical behaviors of radiative and nonradiative recombination processes of the localized excitons, we calculated the temperature dependent variations of radiative and nonradiative recombination lifetimes by the following equations: [16, 17]

$$\tau_{rad} = \tau_{eff} / \eta , \quad (2)$$

$$\eta = I_{emi}(T) / I_{emi}(0) , \quad (3)$$

$$1/\tau_{eff} = 1/\tau_{rad} + 1/\tau_{nr} , \quad (4)$$

Where τ_{rad} and τ_{nr} denote the radiative and nonradiative recombination lifetimes, η is the internal quantum efficiency, $I_{emi}(T)$ and $I_{emi}(0)$ represent the integrated PL emission intensities at temperature T and 0 K, respectively. $I_{emi}(0)$ can't be measured directly, we used $I_{emi}(0) \approx I_{emi}(10\ K)$ as an approximation, this approximation is reasonable since radiative recombination was dominant at 10 K. We obtained the temperature dependence of τ_{rad} and τ_{nr}, as showed in Fig. 6.

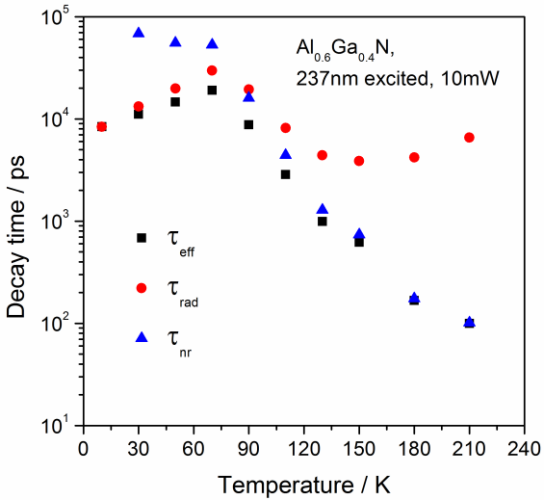

Fig. 6 Temperature dependent PL effective recombination lifetimes, radiative recombination lifetimes and nonradiative recombination lifetimes of E_{P1}.

We can see that τ_{rad} exhibits an anti-S-shaped behavior, increases for 10-70 K, decreases for 70-150 K, and increases again for T >150 K. For T <70 K, we know that carriers are located in the localized states at low temperature from the analysis of temperature dependent PL peak energy of E_{p1}. As we all know, the radiative recombination lifetime of one-dimensional (1D) excitons, two-dimensional (2D) excitons, and three-dimensional (3D) excitons increase with temperature according to $T^{0.5}$, T, and $T^{1.5}$, respectively [18-20], while the radiative recombination lifetime of 0-dimensions (0D) excitons is independent of temperature.[21] Here, we note that τ_{rad} increases almost linearly with temperature

up to 70 K, suggesting that radiative recombination is dominant during this temperature range, what's more, the recombination of localized excitons behaves similarly to 2D excitons. The strong exciton localization will lead to a quantum wells like behavior of light emission, in other words, carries are partly trapped like being confined in quantum wells, and it can effectively suppress the nonradiative processes, resulting in a high efficiency, analogous to the mechanism of luminescence in In GaN-QW LEDs. For 70 K < T <150 K, τ_{rad} decreases as temperature increases, the reason is probably due to the recovery of oscillator strength of electron-hole (*e-h)* pairs in a band-tail. [22] Since at low temperature, carriers are located in the localized states, resulting in a separation of *e-h* wavefunction due to the confinement effect of localized states. As temperature increases, *e-h* pairs begin to be released from the band-tail to 3D space, which can be reflected from the fact that the turnover occurs from the blueshift to redshift for E_{p1} of PL peak energy at 70 K. This leads to increased *e-h* wavefunction overlap and consequently increased oscillator strength. As a result, τ_{rad} decreases with increasing temperature. Meanwhile, τ_{nr} is coming closer and closer to τ_{eff} during this temperature range, implying nonradiative recombination begins to play a more and more important role as temperature increases. For T >150 K, τ_{rad} increases with increasing temperature, we think the reason is that most carriers escape to 3D space due to the increasing thermal energy and consequently the radiative recombination lifetime increasing with temperature according to $T^{1.5}$ becomes dominant. Meanwhile, τ_{nr} is almost equal to τ_{eff}, indicating that nonradiative recombination is dominant during this temperature range.

4. Conclusion

$Al_{0.6}Ga_{0.4}N$ epilayer has been studied by continuous-wave PL and TRPL measurement, and both an S-shaped temperature dependence of PL peak energy shift and an anti-S-shaped temperature dependence of radiative recombination lifetime of carriers were observed. For T<70 K, radiative recombination was dominant, the recombination of localized excitons behaved like quasi 2D excitons that the radiative recombination lifetime increased linearly with temperature. For 70 K <T<150 K, radiative recombination lifetime decreases with increasing temperature due to carriers beginning to be released from the band-tail to 3D space gaining the wavefunction overlap. The relatively slow rising stage of fluorescent decay curve at 70 K is caused by the extended carrier's relaxation process due to carriers transferring. For T>150 K, most carriers escape to 3D space, radiative recombination lifetime increases again as temperature increases, and the recombination processes are dominant by nonradiative recombination. The anti-S-shaped behavior of radiative recombination lifetime is attributed to the competition of carrier's localization and delocalization in the AlGaN alloy.

Acknowledgements

This work was supported by the National Key Research and Development Program of China (Grant No. 2016YFB0400101).

REFERENCES

[1] *G. D. Hao, M. Taniguchi, N. Tamari, and S. Inoue*, J. Phys. D: Appl. Phys. **49**, 235101(2016).
[2] *X. Chen, C. Ji, Y. Xiang, X. Kang, B. Shen, and T. Yu*, Opt. Express. **24**, A935 (2016).
[3] *P. Arivazhagan, R. Ramesh, M. Balaji, K. Asokan, and K. Baskar,* J. Alloys Compd. **679**, 94 (2016).
[4] *X. Jia, D. Chen, L. Bin, H. Lu, R. Zhang, and Y. Zheng*, Sci Rep. **6**, 27728(2016).
[5] *H. Wu, W. Wu, H. Zhang, Y. Chen, Z. Wu, G. Wang, and H. Jiang*, Appl. Phys. Express. **9**, 052103 (2016).
[6] *W. Zhang, J. Xu, W. Ye, Y. Li, Z. Qi, J. Dai, Z. Wu, C. Chen, J. Yin, J. Li, H. Jiang, and Y. Fang*, Appl. Phys. Lett. **106**, 021112(2015).
[7] *E. Kuokstis, W. H. Sun, M. Shatalov, J. W. Yang, and M. A. Khan,* Appl. Phys. Lett. **88**, 261905(2016).
[8] *G. Tamulaitis, I. Yilmaz, M. S. Shur, Q. Fareed, R. Gaska and M. A. Khan*, Appl. Phys. Lett. **85**, 206(2004)
[9] *S. J. Chung, M. S. Kumar, H. J. Lee, and E. K. Suh*, J. Appl. Phys. **95**, 3565(2004)
[10] *K. B. Lee, P. J. Parbrook, T. Wang, F. Ranalli, T. Martin, R. S. Balmer, and D. J. Wallis,* J. Appl. Phys. **101**, 053513(2007).
[11] *J. Li, K. B. Nam, T. N. Oder, K. H. Kim, M. L. Nakarmi, J. Y. Lin, and H. X. Jiang*, Proc. SPIE **4643**, 250(2002).
[12] *H. S. Kim, R. A. Mair, J. Li, J. Y. Lin, and H. X. Jiang*, Appl. Phys. Lett. **76**, 1252(2000).
[13] *Y. H. Cho, G. H. Gainer, J. B. Lam, J. J. Song, W. Yang, W. Jhe*, Phys. Rev. B. **61**, 7203(2000).
[14] *D. Kovalev, B. Averboukh, D. Volm, B. K. Meyer, H. Amano and I. Akasaki*, Phys. Rev. B **54**, 2518(1996).
[15] *N. Nepal, M. L. Nakarmi, K. B. Nam, J. Y. Lin, and H. X. Jiang*, Appl. Phys. Lett. **85**, 2271(2004).
[16] *R. C. Miller, D. A. Kleinman, W. A. Nordland, and A. C. Gossard*, Phys. Rev. B **22**, 863 (1980).
[17] *J. S. Im, A. Moritz, F. Steuber, V. Härle, F. Scholz, and A. Hangleiter,* Appl. Phys. Lett. **70**, 631(1997).
[18] *M. Sugawara*, Phys. Rev. B **51**, 10743(1995).
[19] *H. Akiyama, S. Koshiba, T. Someya, K. Wada, H. Noge, Y. Nahunura, T. Inoshita, A. Shimizu*, Phys. Rev. Lett. **72**, 924(1994).
[20] *J. Feldmann, G. Peter, E. O. Göbel, P. Dawson, K. Moore, C. Foxon, and R. J. Elliott*, Phys. Rev. Lett. **59**, 2337(1987).
[21] *H. Gotoh, H. Ando, T. Takagahara, H. Kamada, A. Chavez-Pirson, and J. Temmyo, Jpn*. J. Appl. Phys. **36**, 4204(1997).
[22] *S. F. Chichibu, T. Onuma, K. Hazu, and A. Uedono*, Appl. Phys. Lett. **97**, 201904 (2010).